J Appl Physiol 108: 1745–1756, 2010.
First published March 4, 2010; doi:10.1152/japplphysiol.00879.2009.

EGCG protects against oxidized LDL-induced endothelial dysfunction by inhibiting LOX-1-mediated signaling

Hsiu-Chung Ou,[1] Tuzz-Ying Song,[2] Yueh-Chiao Yeh,[3] Chih-Yang Huang,[4,5] Shun-Fa Yang,[6] Tsan-Hung Chiu,[7] Kun-Ling Tsai,[8] Kai-Ling Chen,[1] Yun-Jhen Wu,[1] Chiou-Sheng Tsai,[9] Li-Yun Chang,[10] Wei-Wen Kuo,[11]* and Shin-Da Lee[1,12]*

[1]*Department of Physical Therapy and Graduate Institute of Rehabilitation Science, China Medical University, Taichung;* [2]*Department of Nutrition and Health Science, Chungchou Institute of Technology, Changhwa;* [3]*Graduate Institute of Natural Healing Sciences, Nanhua University, Chiayi;* [4]*Graduate Institute of Basic Medical Science, China Medical University, Taichung;* [5]*Department of Health and Nutrition Biotechnology, Asia University, Taichung;* [6]*Institute of Medicine, Chung Shan Medical University, Taichung;* [7]*Department of Obstetrics and Gynecology, China Medical University Hospital, Taichung;* [8]*Graduate Institute of Clinical Medical Science, China Medical University, Taichung;* [9]*Department of Pathology and Laboratory Medicine, Taichung Veterans General Hospital, Taichung;* [10]*Graduate Institute of Molecular Systems Biomedicine,* [11]*Department of Biotechnology, China Medical University, Taichung; and* [12]*Department of Healthcare Administration, Asia University, Taichung, Taiwan*

Submitted 6 August 2009; accepted in final form 10 February 2010

Ou HC, Song TY, Yeh YC, Huang CY, Yang SF, Chiu TH, Tsai KL, Chen KL, Wu YJ, Tsai CS, Chang LY, Kuo WW, Lee SD. EGCG protects against oxidized LDL-induced endothelial dysfunction by inhibiting LOX-1-mediated signaling. *J Appl Physiol* 108: 1745–1756, 2010. First published March 4, 2010; doi:10.1152/japplphysiol.00879.2009.—Lectin-like oxidized low-density lipoprotein receptor-1 (LOX-1), originally identified as the major receptor for oxidized low-density lipoprotein (oxLDL) in endothelial cells, plays a major role in the pathology of vascular diseases. Green tea consumption is associated with reduced cardiovascular mortality in some epidemiological studies. In the present study, we hypothesized that the most abundant polyphenolic compound in tea, epigallocatechin-3-gallate (EGCG), can downregulate parameters of endothelial dysfunction by modulating LOX-1-regulated cell signaling. In cultured human umbilical vein endothelial cells (HUVECs), exposure to oxLDL (130 μg/ml), which led to an increase in LOX-1 expression at the RNA and protein levels, was abrogated by addition of EGCG or DPI, a well-known inhibitor of flavoproteins, suggesting the involvement of NADPH oxidase. Furthermore, oxLDL rapidly activated the membrane translocation of Rac-1 and $p47^{phox}$ and the subsequent induction of ROS generation, which was suppressed markedly by pretreatment with EGCG or anti-LOX-1 monoclonal antibody. OxLDL also increased p38 MAPK phosphorylation and decreased phosphorylation of the amino-terminal region of Akt, with maximal induction at about 30 min, and NF-κB phosphorylation within 1 h, resulting in redox-sensitive signaling. In addition, oxLDL diminished the expression of endothelial nitric oxide synthase (eNOS), enhanced the expression of endothelin-1 and adhesion molecules (ICAM, E-selectin, and monocyte chemoattractant protein-1), and increased the adherence of monocytic THP-1 cells to HUVECs. Pretreatment with EGCG, however, exerted significant cytoprotective effects in all events. These data suggest that EGCG inhibits the oxLDL-induced LOX-1-mediated signaling pathway, at least in part, by inhibiting NADPH oxidase and consequent ROS-enhanced LOX-1 expression, which contributes to further ROS generation and the subsequent activation of NF-κB via the p38 MAPK pathway. Results from this study may provide insight into a possible molecular mechanism by which EGCG suppresses oxLDL-mediated vascular endothelial dysfunction.

lectin-like oxidized low-density lipoprotein receptor-1; adhesion molecule; inflammation; nicotinamide adenine dinucleotide phosphate oxidase; reactive oxygen species

OXIDATIVE STRESS AND SUPEROXIDE ANION GENERATION are believed to play important roles in the pathogenesis of various cardiovascular diseases, including arteriosclerosis. Under oxidative stress, low-density lipoprotein (LDL) particles trapped in the vessel wall become oxidized. The resulting oxidized LDL (oxLDL) causes activation, followed by dysfunction of endothelium. Various enzymatic origins of reactive oxygen species (ROS) in the vasculature have been proposed, including xanthine oxidase, myeloperoxidase, lipoxygenase, and nicotinamide adenine dinucleotide phosphate (NADPH) oxidase. Furthermore, ROS can regulate the expression of redox-sensitive vascular genes such as chemokines and adhesion molecules by changing the redox state of endothelial cells (33). These molecules facilitate the adhesion of monocytes to endothelial cells, thereby initiating atherosclerosis.

The major source of intracellular ROS in vascular cells is NADPH oxidase, a multisubunit enzymatic complex comprising two membrane-bound subunits, gp91 and $p22^{phox}$. Assembly of the active complex is regulated by cytoplasmic subunits such as $p47^{phox}$, $p67^{phox}$, and a low-molecular G protein, Rac-1 (1). A recent study indicated that the activation of Rac-1 and $p47^{phox}$ is involved in the generation of superoxide, a molecule that stimulates inflammatory gene expression through a redox-sensitive signaling pathway in vascular endothelial cells (43). These findings strongly suggest that both $p47^{phox}$ and Rac-1 are critical components of endothelial NADPH oxidase.

LOX-1, a lectin-like receptor for oxLDL, is present on endothelial cells (50). In vascular endothelial cells, LOX-1 activation has been suggested to induce several intracellular signaling pathways, including the activation of NADPH oxidase on the cell membrane, resulting in the quick increase of intracellular ROS, including O_2^- and H_2O_2 (8). Increased levels of O_2^- can react with intracellular NO, resulting in the decrease of intracellular NO (12) and the activation of p38 (MAPK) (35), protein kinase B (27), transcription factor NF-κB, and subsequent downstream inflammatory responses (11). These

* W.-W. Kuo and S.-D. Lee contributed equally to this work.
Address for reprint requests and other correspondence: S.-D. Lee, Dept. of Physical Therapy, Graduate Institute of Rehabilitation Science, China Medical Univ., 91 Hsueh-Shih Road, Taichung 40202, Taiwan (e-mail: shinda@mail.cmu.edu.tw).

activations are attenuated by pretreating cells with a specific LOX-1 antibody or antisense LOX-1 mRNA (6, 8).

Green tea (*Camellia sinensis*) has only recently been studied extensively for its beneficial health effects (5). Numerous epidemiological studies have reported an inverse relationship between tea consumption and cardiovascular events (46), and this phenomenon may be associated with the antioxidant capacity of components of green tea to scavenge various types of radicals in aqueous and organic environments (53). Green tea is chemically characterized by the presence of high amounts of polyphenolic compounds known as catechins, the most abundant of which is epigallocatechin-3-gallate (EGCG). EGCG has been reported to possess both anti-inflammatory and antiatherogenic properties in experimental studies conducted in vitro and in vivo (16, 31, 57). It also has been hypothesized that the antiatherosclerotic activity of EGCG is associated with its antioxidative activity. Substantial evidence suggests that EGCG acts as an antioxidant by attenuating lipid peroxidation caused by various forms of ROS (19), thereby reducing the expression of the endogenous NO synthase inhibitor asymmetric dimethyl arginine (52) as well as reducing the expression of cytokine-induced vascular adhesion molecule-1 (31). Whether EGCG influences oxLDL-induced NADPH oxidase expression and related downstream signaling pathways by inhibiting the expression of LOX-1 is not clear. Since endothelial NADPH oxidase is the major contributor to ROS production in vascular walls, and oxidative stress is believed to be implicated in aberrant behavior of the vascular endothelium and the pathogenesis of cardiovascular disease, we therefore sought to examine how EGCG regulates endothelial NADPH oxidase-mediated downstream signaling caused by oxLDL and whether such regulation correlates with an effect on LOX-1 expression.

MATERIALS AND METHODS

Reagents. Fetal bovine serum, medium 199 (M199), and trypsin-EDTA were obtained from GIBCO (Grand Island, NY); low-serum growth supplement was obtained from Cascade (Portland, OR); and 2′,7′-bis-2-carboxyethyl-5(6)-carboxyfluorescein acetoxymethyl ester (BCECF-AM), diphenylene iodonium (DPI), EGCG, penicillin, and streptomycin were obtained from Sigma (St. Louis, MO). Dihydroethidium (DHE) was purchased from Molecular Probes (Eugene, OR); anti-LOX-1, anti-monocyte chemoattractant protein-1 (MCP-1), anti-intercellular adhesion molecules (ICAM), anti-E-selectin, IL-8, and ET-1 ELISA kits were purchased from R&D Systems (Minneapolis, MN). Anti-Cu, Zn superoxide dismutase (SOD-1) and anti-Mn superoxide dismutase (SOD-2) were obtained from Santa Cruz Biotechnology (Santa Cruz, CA); anti-NF-κB/p65, anti-IκBα, anti-endothelial NO synthase (eNOS) were obtained from Transduction Laboratories (San Jose, CA); anti-Rac-1 and anti-$p47^{phox}$ were obtained from BD Biosciences (Piscataway, NJ); and anti-cyclooxygenase-2 (COX-2) was obtained from Chemicon (Billerica, MA).

Cell cultures. This experiment was approved by the Research Ethics Committee of the China Medical University Hospital. After receiving written consent from the parents, we obtained fresh human umbilical cords from normal full-term neonates shortly after birth and suspended them in Hanks' balanced salt solution (HBSS; GIBCO) at 4°C. Human umbilical vein endothelial cells (HUVECs) were isolated from human umbilical cords with collagenase and used at *passages 2* and *3* as previously described (44). After dissociation, the cells were collected and cultured on gelatin-coated culture dishes in M199 with low-serum growth supplement, 100 IU/ml penicillin, and 0.1 mg/ml streptomycin. Subcultures were performed with trypsin-EDTA. Media were refreshed every 2 days. The identity of umbilical vein endothelial cells was confirmed by their cobblestone morphology and strong positive immunoreactivity to von Willebrand factor. THP-1, a human monocytic leukemia cell line, was obtained from ATCC (Rockville, MD) and cultured in RPMI with 10% FBS at a density of 2–5 $\times$ 10^6 cells/ml as suggested in the product specification sheet provided by the vendor.

Lipoprotein separation. Human plasma was obtained from the Taichung Blood Bank (Taichung, Taiwan), and LDL was isolated using sequential ultracentrifugation (ρ = 1.019–1.210 g/ml) in KBr solution containing 30 mM EDTA, stored at 4°C in a sterile, dark environment, and used within 3 days as previously described (20). Immediately before the oxidation tests, LDL was separated from EDTA and from diffusible low-molecular-mass compounds by gel filtration on PD-10 Sephadex G-25 M gel (Pharmacia) in 0.01 M phosphate-buffered saline (PBS: 136.9 mM NaCl, 2.68 mM KCl, 4 mM Na_2HPO_4, and 1.76 mM KH_2PO_4) at pH 7.4. Cu^{2+}-modified LDL (1 mg protein/ml) was prepared by exposing LDL to 10 μM $CuSO_4$ for 16 h at 37°C. Protein was measured using the Bradford method (3).

Isolation of mRNA and real-time PCR. Total RNA was isolated from the HUVECs using the RNeasy kit (Qiagen, Valencia, CA). Oligonucleotides (LOX-1, β-actin) were designed using the computer software package Primer Express 2.0 (Applied Biosystems, Foster City, CA). All oligonucleotides were synthesized by Invitrogen (Breda, The Netherlands). Oligonucleotide specificity was computer tested (BLAST, National Center for Biotechnology Information, Bethesda, MD) by homology search with the human genome and later confirmed by dissociation curve analysis. The oligonucleotide sequences were as follows: LOX-1 sense primer, 5′-GATGCCCCACTTGTTCAGAT-3′; antisense primer, 5′-CAGAGTTCGCACCTACGTCA-3′; β-actin sense primer, 5′-AGGTCATCACTATTGGCAACGA-3′; antisense primer, 5′-CACTTCATGATGGAATTGAATGTAGTT-3′. PCRs were performed using the SYBR Green method in an ABI 7000 sequence detection system (Applied Biosystems) according to the manufacturer's guidelines. The reactions were set by mixing 12.5 μl of the SYBR Green Master Mix (Applied Biosystems) with 1 μl of a solution containing 5 nmol/μl of both oligonucleotides, and 1 μl of a cDNA solution (1/100 of the cDNA synthesis product). The cycle threshold (Ct) value was defined as the number of PCR cycles required for the fluorescence signal to exceed the detection threshold value (fixed at 0.2 relative fluorescence units). This threshold was set constant throughout the study and corresponded to the log linear range of the amplification curve.

Measurement of ROS production. The effect of EGCG on ROS production in HUVECs was determined by performing a fluorometric assay, using DHE as a probe for the presence of superoxide. After preincubation for 2 h with the indicated concentrations of EGCG, HUVECs were incubated with DHE for 1 h, followed by incubation with oxLDL for 2 h. The fluorescence intensity was measured at 540-nm excitation and 590-nm emission (before and after exposure to oxLDL) using a fluorescence microplate reader (Labsystems, Mountain View, CA). The percent increase in fluorescence per well was calculated using the formula $[(Ft_2 - Ft_0)/Ft_0] \times 100$, where Ft_2 is the fluorescence at 2 h of oxLDL exposure and Ft_0 is the fluorescence at 0 min of oxLDL exposure. To evaluate the role of NADPH oxidase and LOX-1 in oxLDL-induced ROS generation, we preincubated cells with the flavoprotein inhibitor DPI (5 μM) and anti-LOX-1 monoclonal antibody (mAb; 40 μg/ml) for 2 h before exposure to oxLDL.

Preparation of nuclear and cytosolic extracts. Nuclear and cytosolic extracts were isolated with a Nuclear and Cytoplasmic Extraction kit (Pierce Chemical, Rockford, IL). After the incubation period, HUVECs were collected by centrifugation at 600 *g* for 5 min at 4°C. The pellets were washed twice with ice-cold PBS, followed by the addition of 0.2 ml of cytoplasmic extraction *buffer A* and vigorous mixing for 15 s. Ice-cold cytoplasmic extraction *buffer B* (11 μl) was added to the solution. After vortex mixing, nuclei and cytosolic fractions were separated by centrifugation at 16,000 *g* for 5 min. The cytoplasmic extracts (supernatants) were stored at −80°C. Nuclear

extraction buffer was added to the nuclear fractions (pellets), which were then mixed by vortex mixing on the highest setting for 15 s. The mixture was iced, and a 15-s vortex was performed every 10 min for a total of 40 min. Nuclei were centrifuged at 16,000 *g* for 10 min. The nuclear extracts (supernatants) were stored at −80°C until use.

Preparation of membrane and cytosolic extracts. A cellular membrane fraction was prepared with Mem-PER (Pierce) according to the manufacturer's instructions. The Mem-PER system consists of three reagents: reagent A is a cell lysis buffer, reagent B is a detergent dilution buffer, and reagent C is a membrane solubilization buffer. After the incubation period, HUVECs were collected by centrifugation at 600 *g* for 5 min at 4°C. Each cell pellet, containing 5×10^6 cells, was lysed at room temperature using Mem-PER reagent A. Membrane proteins were solubilized on ice with Mem-PER reagent C diluted 2:1 with Mem-PER reagent B. Reagents A and B/C were supplemented with Halt protease inhibitor cocktail (Pierce Biotechnology). The solubilized protein mixture was centrifuged at 10,000 *g* for 3 min at 4°C to remove cellular debris. The clarified supernatant was heated at 37°C for 10 min, followed by centrifugation at 10,000 *g* for 2 min to produce separated membrane and hydrophilic protein fractions. The hydrophobic fraction of membrane proteins (bottom layer) was stored at −80°C until use.

Immunoblotting. To determine whether EGCG could ameliorate the oxLDL-induced apoptosis-regulating proteins, we grew HUVECs to confluence, pretreated cells with EGCG for 2 h, and then stimulated cells with oxLDL for 24 h. After treatment, cytosolic and membrane protein fractions as well as cytosolic and nucleic protein fractions of cells were extracted. Cytosolic p38, Akt, SOD-1, SOD-2, eNOS, COX-2, IκBα, and membrane $p47^{phox}$ and Rac-1 as well as nucleic NF-κB p65 expressions were determined by SDS-PAGE and immunoblot assay. The blots was incubated with blocking buffer (1× PBS and 5% nonfat dry milk) for 1 h at room temperature and then probed with primary antibodies (1:1,000 dilutions) overnight at 4°C, followed by incubation with horseradish peroxidase-conjugated secondary antibody (1:5,000) for 1 h. To control equal loading of total protein in all lanes, we stained blots with mouse anti-β-actin antibody at a 1:50,000 dilution. The bound immunoproteins were detected by an enhanced chemiluminescence assay (ECL; Amersham, Little Chalfont, UK). The intensities were quantified by densitometric analysis (Digital Protein DNA Imagineware, Huntington Station, NY).

Assay for IL-8 and ET-1 secretion. HUVECs were seeded in 24-well plates at 0.5×10^5 cells. After 2 days, cells were pretreated with the indicated concentrations of EGCG for 2 h, followed by treatment with oxLDL (130 μg/ml) for 24 h. At the end of the oxLDL incubation period, cell supernatants were removed and assayed for IL-8 and ET-1 concentration using an ELISA kit obtained from R&D Systems. Data are expressed in nanograms per milliliter of duplicate samples.

Measurement of intracellular Ca^{2+} concentration. To determine the effect of EGCG on the rise of oxLDL-induced intracellular Ca^{2+} concentration ($[Ca^{2+}]_i$), we seeded HUVECs onto 24-mm glass coverslips, pretreated cells with EGCG for 2 h, and then stimulated cells with oxLDL (130 μg/ml) for the indicated time periods. The cells on the coverslips were loaded with 2 μM fura-2 AM (Molecular Probes) in M199 and allowed to stand for 30 min at 37°C. After being loaded, the cells were washed with HEPES buffer (in mM: 131 NaCl, 5 KCl, 1.3 $CaCl_2$, 1.3 Mg_2SO_4, 0.4 KH_2PO_4, 20 HEPES, and 25 glucose, pH 7.4) to remove excess fluorescent dye. The fluorescence of the cells on each coverslip was then measured and recorded using an inverted Olympus IX-70 microscope. $[Ca^{2+}]_i$ in endothelial cells was monitored at an emission wavelength of 510 nm with excitation wavelengths alternating between 340 and 380 nm using a Delta Scan System (Photon Technology International, Princeton, NJ) and was calculated using Grynkiewicz's method (18).

Adhesion assay. HUVECs at 1×10^5 cells/ml were cultured in 96-well flat-bottom plates (0.1 ml/well) for 1–2 days. Cells were then pretreated with the indicated concentrations of EGCG for 2 h and incubated with oxLDL (130 μg/ml) for 24 h. The medium was then removed, and 0.1 ml/well of THP-1 cells (prelabeled with 4 μM BCECF-AM for 30 min in RPMI at a density of 1×10^6 cells/ml) was added in RPMI. The cells were allowed to adhere at 37°C for 1 h in a 5% CO_2 incubator. The nonadherent cells were removed by gentle aspiration. Plates were washed three times with M199. The number of adherent cells was estimated by microscopic examination; the cells were then lysed with 0.1 ml of 0.25% Triton X-100. The fluorescence intensity was measured at 485-nm excitation and 538-nm emission using a fluorescence microplate reader (Labsystems).

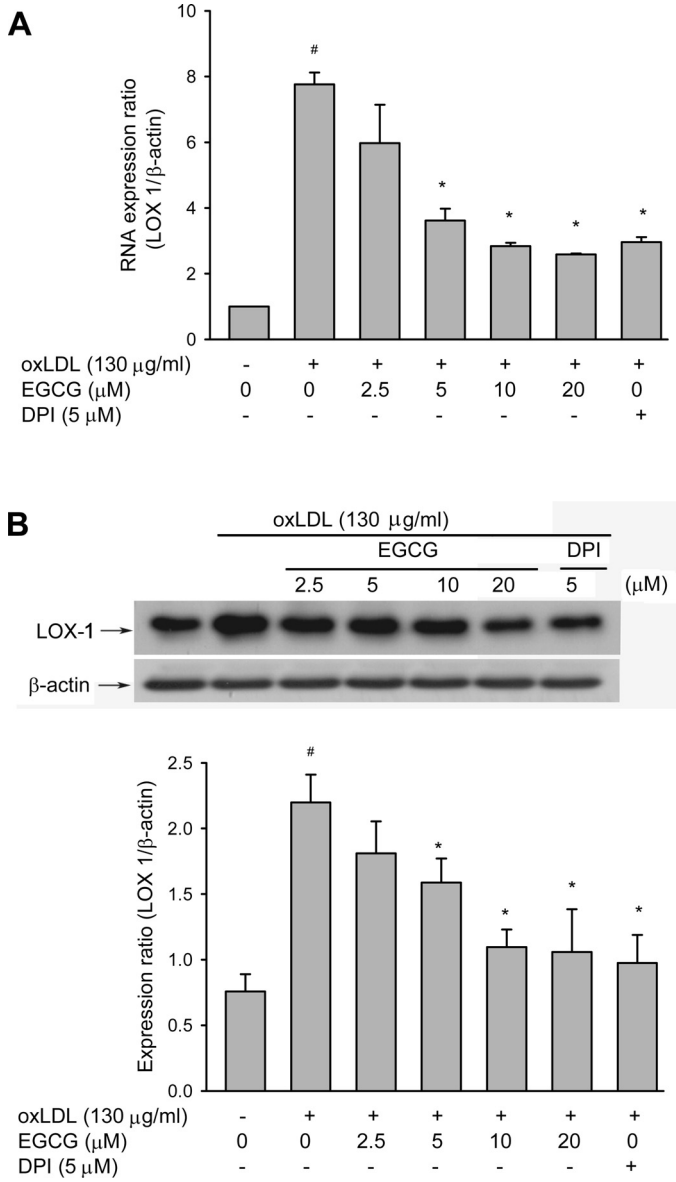

Fig. 1. Inhibitory effect of epigallocatechin-3-gallate (EGCG) on oxidized LDL (oxLDL)-induced endothelial lectin-like oxLDL receptor-1 (LOX-1) gene (*A*) and protein expression (*B*). Human umbilical vein endothelial cells (HUVECs) were pretreated with EGCG (2.5–20 μM) or diphenylene iodonium (DPI; 5 μM) for 2 h, followed by exposure to oxLDL (130 μg/ml) for a further 24 h. At the end of the incubation period, cells were lysed and LOX-1 mRNA and protein were analyzed by real-time PCR and Western blotting, respectively. Both mRNA and protein levels of LOX-1 were normalized to the level of β-actin. Data are means ± SE of 3 different experiments. #$P < 0.05$ compared with untreated control HUVECs. *$P < 0.05$ compared with oxLDL-stimulated HUVECs.

Adhesion molecule expression. To determine whether EGCG could modify oxLDL-induced adhesion molecule expression, we grew HUVECs to confluence, pretreated cells with EGCG for 2 h, and stimulated cells with oxLDL (130 μg/ml) for 24 h. At the end of stimulation, HUVECs were harvested and incubated with FITC-conjugated anti-ICAM-1, anti-E-selectin, and anti-MCP-1 (R&D Systems) for 45 min at room temperature. After the HUVECs had been washed three times, their immunofluorescence intensity was analyzed by flow cytometry using a Becton Dickinson FACScan flow cytometer (Mountain View, CA).

Statistical analyses. Results are means ± SE. Differences between the groups were analyzed using one-way ANOVA followed by Student's *t*-test. A P value <0.05 was considered statistically significant.

RESULTS

Modulation of oxLDL-induced LOX-1 expression by EGCG. It has been shown that oxLDL increases LOX-1 expression (mRNA and protein) (26). Incubation of HUVECs with oxLDL (130 μg/ml) enhanced LOX-1 expression at both the gene (Fig. 1*A*) and protein levels (Fig. 1*B*). Treatment of HUVECs with EGCG for 2 h before exposure to oxLDL for 24 h resulted in suppression of LOX-1 expression in a dose-dependent manner. Notably, pretreatment with DPI, an inhibitor of ROS production, markedly inhibited oxLDL-induced LOX-1 upregulation, strongly suggesting that ROS plays a critical role in the increased expression of LOX-1.

EGCG inhibited oxLDL-induced ROS generation in HUVECs. Next, we used fluorescence microscopy to analyze the effect of EGCG on the LOX-1-mediated redox-sensitive signaling pathway in endothelial cells. The level of ROS generation in endothelial cells pretreated with EGCG (2.5–20 μM) for 2 h followed by exposure to 130 μg/ml oxLDL decreased in a dose-dependent manner (all $P < 0.05$) (Fig. 2, *A* and *B*). In addition, oxLDL-induced ROS was abrogated by pretreatment with monoclonal antibody of LOX-1 (anti-LOX-1 mAb) or DPI (Fig. 2*B*), suggesting that ROS generation, one of the earliest signals after oxLDL exposure, was largely dependent on the binding of oxLDL to LOX-1 and subsequent activation of NADPH oxidase. Intracellular ROS levels are regulated by the balance between ROS generation and the activity of antioxidant enzymes such as SOD and catalase. The H_2O_2 generated by superoxide dismutation is able to inactivate SOD, thereby increasing the imbalance in favor of oxidative stress. We therefore measured the expression levels of SOD and its isoforms in endothelial cells in response to oxLDL. Our results showed that SOD-1, but not SOD-2, expression was diminished after treatment with oxLDL for 24 h and could be significantly rescued by pretreatment with EGCG (Fig. 2, *C* and *D*).

EGCG inhibited membrane translocation of p47^{phox} and Rac-1. Endothelial NADPH oxidase is a major source of ROS in vascular endothelial cells, and atherogenic levels of LDL

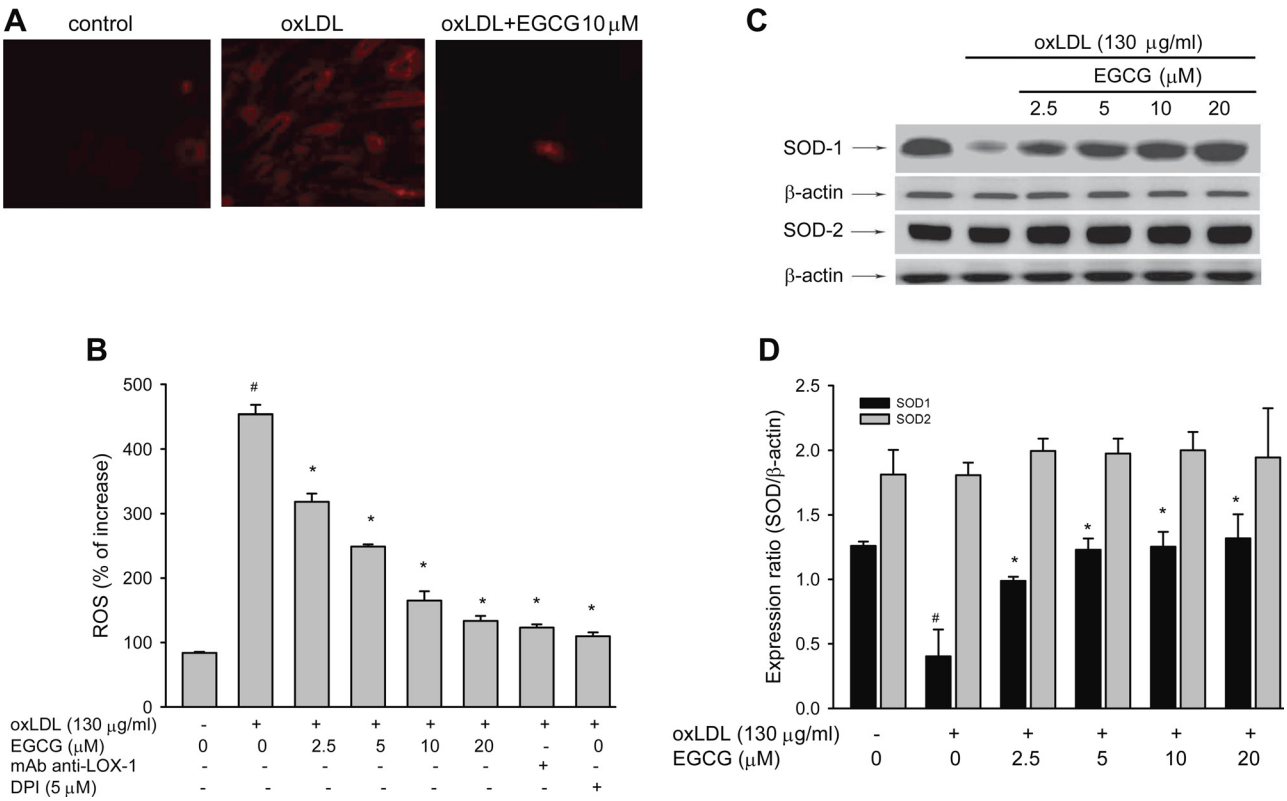

Fig. 2. Inhibitory effects of EGCG on oxLDL-induced ROS production in HUVECs. After preincubation for 2 h with 2.5–20 μM EGCG or anti-LOX-1 monoclonal antibody (mAb; 40 μg/ml) followed by a 1-h incubation with the fluorescent probe dihydroethidium (DHE; 10 μM), 130 μg/ml oxLDL was then added to the medium for 2 h. *A*: fluorescence intensity of cells measured by fluorescence microcopy. *B*: fluorescence distribution of DHE oxidation expressed as a percentage of increased intensity. *C* and *D*: representative Western blots of Cu,Zn-SOD (SOD-1) and Mn-SOD (SOD-2) protein levels in HUVECs pretreated with EGCG for 2 h followed by 130 μg/ml oxLDL for 24 h. Data are means ± SE of 3 independent analyses. #$P < 0.05$ compared with untreated control HUVECs. *$P < 0.05$ compared with oxLDL-stimulated HUVECs.

have been shown to induce a marked increase in NADPH oxidase-generated ROS by the endothelium (49). Since active NADPH oxidase is assembled on the membrane, the effects of EGCG on membrane translocation of $p47^{phox}$ and Rac-1 were examined by Western blotting. Figure 3 shows that the levels of membrane-bound $p47^{phox}$ and Rac-1 were approximately two- to threefold higher in cells treated with oxLDL for 30 min than in untreated cells. This effect was inhibited by pretreatment with EGCG in a dose-dependent manner (all $P < 0.05$).

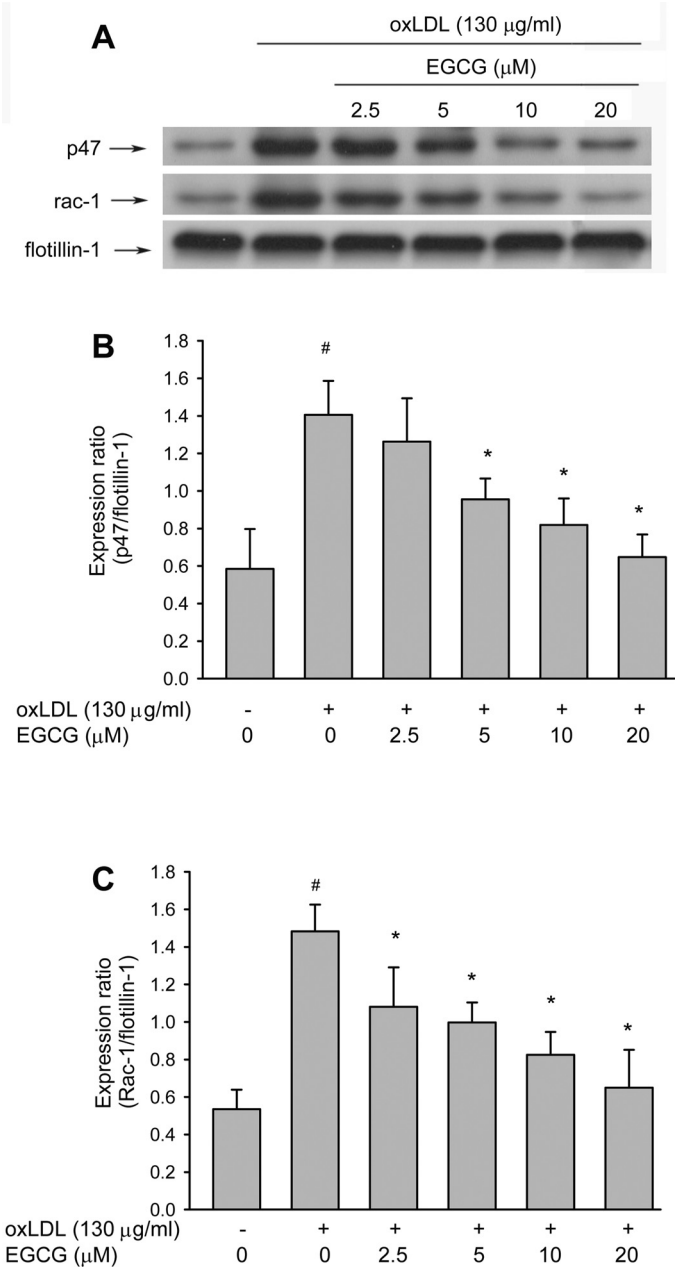

Fig. 3. Effects of EGCG on oxLDL-induced $p47^{phox}$ and Rac-1 membrane translocation. HUVECs were pretreated with indicated concentrations of EGCG (2.5–20 μM) for 2 h followed by 130 μg/ml oxLDL for 30 min. Representative Western blots (*A*) and summary data (*B* and *C*) show that EGCG protected against oxLDL-induced $p47^{phox}$ and Rac-1 translocation to the plasma membrane. Anti-flotillin-1 antibody was used for normalization of membrane proteins. Data are means ± SE of 3 independent analyses. #$P <$ 0.05 compared with untreated control HUVECs. *$P < 0.05$ compared with oxLDL-stimulated HUVECs.

EGCG inhibited NF-κB activation via modulation of p38 MAPK and Akt phosphorylation. OxLDL-induced ROS can activate two signal transduction pathways involving either p38 MAPK or phosphoinositide 3-kinase (PI3K), both causing NF-κB activation, which facilitates nuclear translocation and subsequent regulation of proinflammatory gene expression (9). As shown in Fig. 4*A*, incubation of HUVECs with oxLDL resulted in significant phosphorylation of p38 MAPK and dephosphorylation of Akt (a downstream effector of PI3K) within 30 min without affecting their protein levels; this tendency was reversed significantly with EGCG pretreatment. The inhibitor protein IκBα regulates the transcriptional activity of NF-κB p65. In resting cells, IκBα binding masks the NF-κB nuclear localization sequence, sequestering the complex in the cytosol. The key step in NF-κB nuclear translocation is mediated by degradation of cytosolic IκBα. Therefore, we used immunoblotting to examine the effect of EGCG on protein levels of NF-κB p65 and IκBα in nuclear and cytosol extracts. The results showed that in HUVECs exposed to oxLDL (130 μg/ml, 1 h), the protein levels of NF-κB p65 in the nuclear fraction increased and the levels of IκBα in cytosol decreased. In cells pretreated with EGCG (2.5–20 μM), the nuclear translocation of NF-κB p65 protein decreased in a dose-dependent manner ($P < 0.05$) (Fig. 4, *D–F*).

EGCG suppressed oxLDL-induced NF-κB-related gene products. Activation of NF-κB is a multistep process including IκB phosphorylation. Phosphorylated IκB liberates NF-κB, which is then transferred from the cytoplasm to the nucleus, where it activates the transcription of various inflammatory cytokines, genes encoding COX-2, and cell adhesion molecules. Therefore, we sought to determine whether EGCG inhibits oxLDL-induced expression of COX-2 and other inflammatory molecules. We found that COX-2 expression (Fig. 5*A*) and IL-8 secretion (Fig. 5*B*) were increased in cells exposed to oxLDL. As expected, pretreatment with EGCG significantly inhibited both COX-2 expression and IL-8 secretion in a dose-dependent manner (all $P < 0.05$).

EGCG ameliorated oxLDL-diminished eNOS protein expression and enhanced ET-1 secretion. OxLDL has been shown to reduce the expression of eNOS and enhance the secretion of ET-1 via ROS generation, thereby altering endothelial biology (56). We examine the effect of EGCG on the protein levels of eNOS and ET-1 secretion caused by oxLDL. Our results showed that oxLDL significantly reduced eNOS protein expression (47%, $P < 0.05$) (Fig. 6*A*) and enhanced ET-1 secretion (30.8 ± 1.2 and 72.3 ± 3.2 pg/ml for control and oxLDL, respectively, $P < 0.05$) in HUVECs after 24 h of incubation. This tendency was reversed significantly, however, in cells pretreated with EGCG (Fig. 6).

EGCG inhibited oxLDL-induced $[Ca^{2+}]_i$ rise. The recent findings (43) that blockade of Ca^{2+} inhibits Rac-1 and $p47^{phox}$ activation and ROS generation in endothelial cells and that blockade of NADPH oxidase and ROS generation suppresses Ca^{2+} signaling prompted us to examine whether EGCG affects the level of oxLDL-induced intracellular Ca^{2+} in endothelial cells. As shown in Fig. 7, the basal level of intracellular Ca^{2+} increased in oxLDL-treated cells after 24 h, whereas EGCG significantly inhibited the oxLDL-induced rise in intracellular Ca^{2+} (all $P < 0.05$).

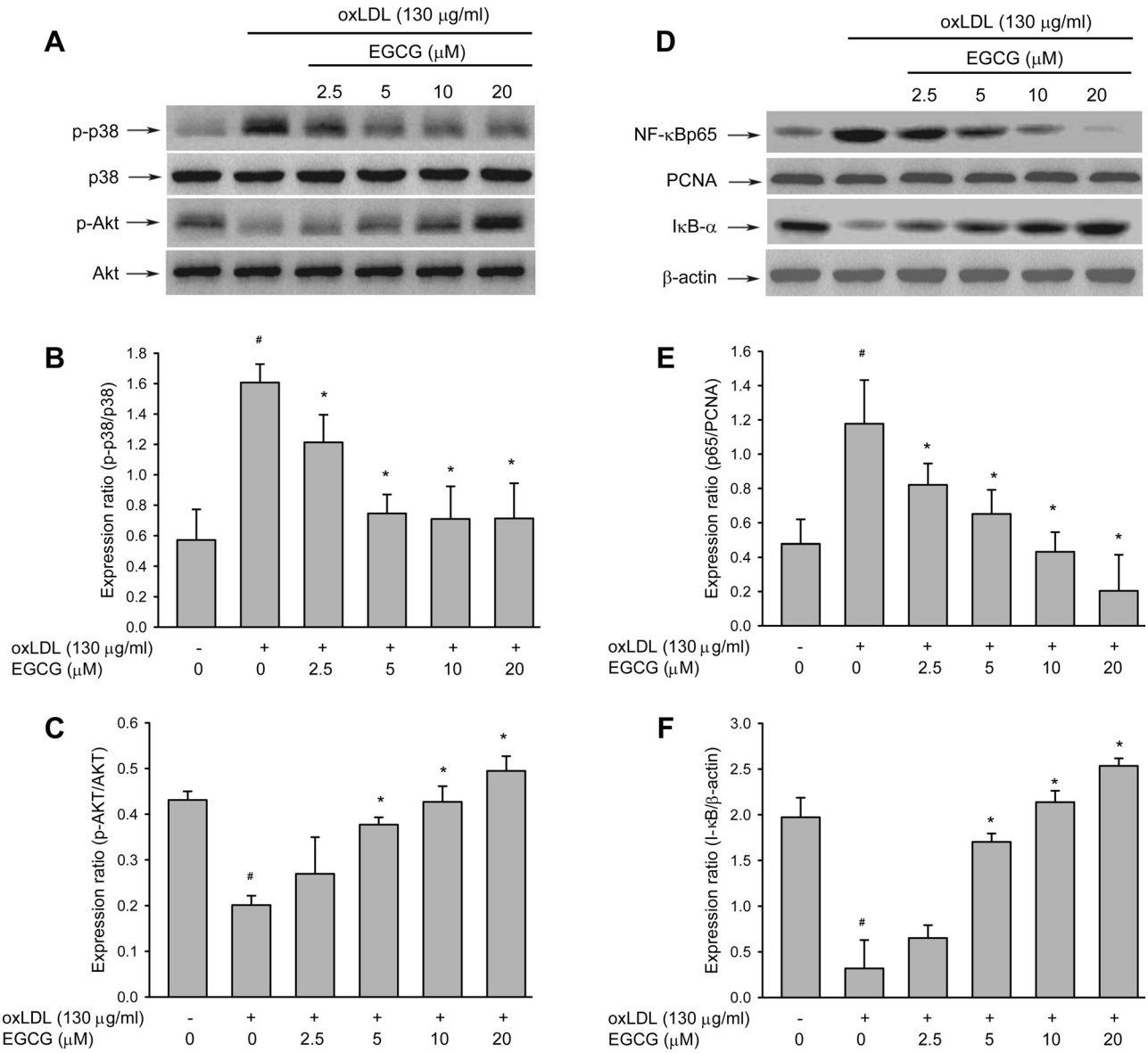

Fig. 4. Effects of EGCG on phosphorylation of p38 MAPK and Akt and on the translocation of NF-κB. HUVECs were pretreated with indicated concentrations of EGCG for 2 h followed by exposure to 130 μg/ml oxLDL for 30 min. Western blot analysis was used to evaluate the expression of both phosphorylated and total p38 MAPK and Akt (*A–C*) after 30 min of exposure and the activation of NF-κB (*D–F*) after 60 min of exposure. Anti-β-actin and anti-PCNA antibodies were used for normalization of cytosolic and nuclear proteins, respectively. Values are means ± SE of 3 independent analyses. #$P < 0.05$ compared with untreated control HUVECs. *$P < 0.05$ vs. oxLDL treatment.

EGCG suppressed the oxLDL-induced adherence of THP-1 cells to HUVECs and expression of adhesion molecules. OxLDL-enhanced recruitment, retention, and adhesiveness of human monocytes and monocytic cell lines to endothelium has been implicated in the initial stage of atherogenesis (24). To test the effect of EGCG on monocyte adhesion to HUVECs, we pretreated confluent monolayers of HUVECs with various concentrations of EGCG for 2 h and then stimulated them with oxLDL (130 μg/ml) for 24 h, followed by incubation with THP-1 cells for 1 h at 37°C. As shown in Fig. 8, *A* and *B*, oxLDL stimulated an increase in adherence of THP-1 cells to HUVECs (223 ± 11%, $P < 0.05$); however, the effect was significantly inhibited by EGCG treatment in a dose-dependent manner (all $P < 0.05$). The effect of EGCG on the surface expression of adhesion molecules on HUVECs exposed to oxLDL was subsequently examined. As shown in Fig. 8*C*, the expression levels of ICAM-1, E-selectin, and MCP-1 were significantly higher in HUVECs that had been treated with oxLDL (130 μg/ml) for 24 h than in the control cells (176, 490, and 262%, respectively, compared with control). Flow cytometry revealed that the induction of adhesion molecule expression was significantly ameliorated by the presence of 10 μM EGCG (all $P < 0.05$).

DISCUSSION

LOX-1 is expressed in endothelial cells, smooth muscle cells, and macrophages. It is believed to be the main receptor for oxLDL and hence to play an important role in the pathogenesis of atherosclerosis (36). The binding of oxLDL to

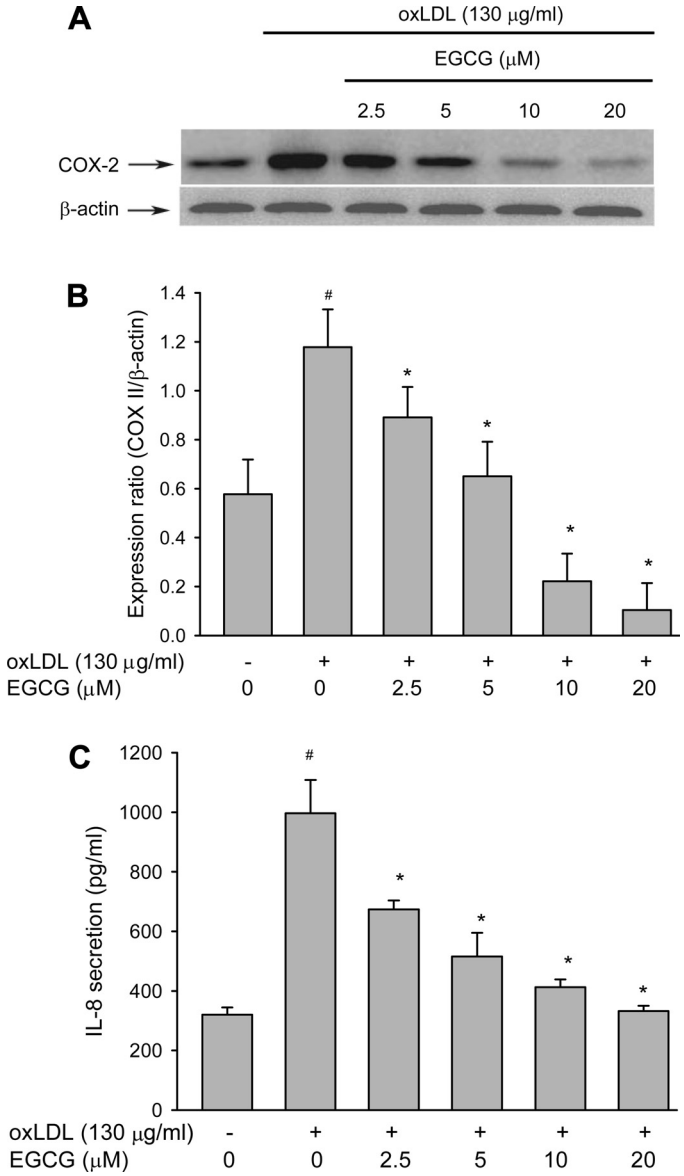

Fig. 5. Effects of EGCG on oxLDL-induced cyclooxygenase-2 (COX-2) expression (*A* and *B*) and IL-8 secretion (*C*) through NF-κB activation. HUVECs were pretreated for 2 h with the indicated concentrations of EGCG followed by oxLDL (130 μg/ml) for 24 h. For Western blot analyses, a monoclonal anti-COX-2 antibody and a monoclonal anti-β-actin antibody (for normalization) were used. Values are means ± SE of 3 independent analyses. #$P < 0.05$ compared with untreated control HUVECs. *$P < 0.05$ vs. oxLDL treatment.

LOX-1 initiates ROS formation, which in turn upregulates LOX-1 expression, thereby contributing to further ROS generation (8). The present study is the first to show the effectiveness of EGCG, the most abundant catechin in green tea, in suppressing endothelial LOX-1 expression and LOX-1-mediated proatherogenic effects. This effect of EGCG on endothelial LOX-1 expression appears to be exerted at the transcriptional level, as reflected by the parallel decrease in LOX-1 mRNA and protein levels in EGCG-treated cells (Fig. 1). Furthermore, pretreatment with DPI or blockade of LOX-1 with anti-LOX-1 mAb prevented oxLDL-induced ROS generation, which suggests that the binding of oxLDL to LOX-1 and the consequent formation of ROS may be the first event in LOX-1-mediated endothelial dysfunction (Fig. 2). Because regulation of LOX-1 gene expression is redox sensitive (38) and involves NF-κB (14), suppression of oxLDL-induced ROS production by EGCG may contribute to the reduction of LOX-1-mediated activation of NF-κB and related expression of a number of proinflammatory molecules.

It has been shown that oxLDL-induced endothelial dysfunction is caused by an increase in NADPH oxidase-generated superoxide concentrations and a decrease in antioxidative enzyme activity (48), resulting in the activation of multiple

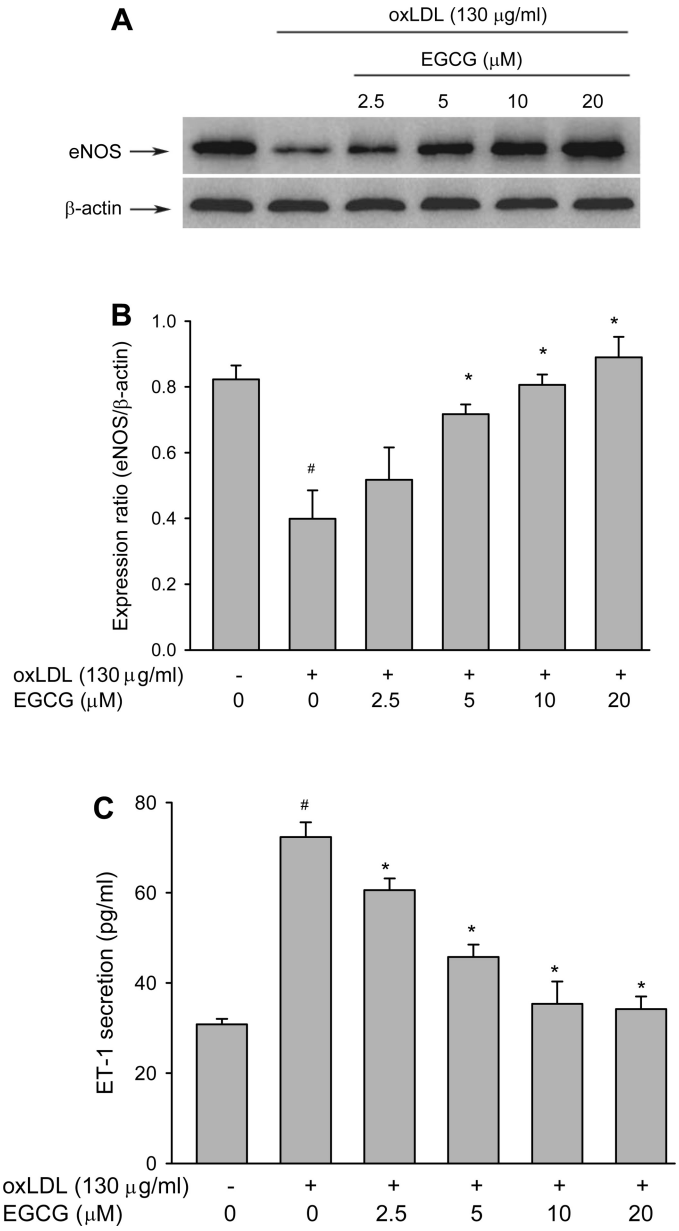

Fig. 6. Effects of EGCG on endothelial nitric oxide synthase (eNOS) expression (*A* and *B*) and ET-1 secretion (*C*) caused by oxLDL. HUVECs were pretreated for 2 h with the indicated concentrations of EGCG followed by oxLDL (130 μg/ml) for 24 h. For Western blot analyses, a monoclonal anti-eNOS antibody and a monoclonal anti-β-actin antibody (for normalization) were used. Values are means ± SE of 3 independent analyses. #$P < 0.05$ compared with untreated control HUVECs; *$P < 0.05$ vs. oxLDL treatment.

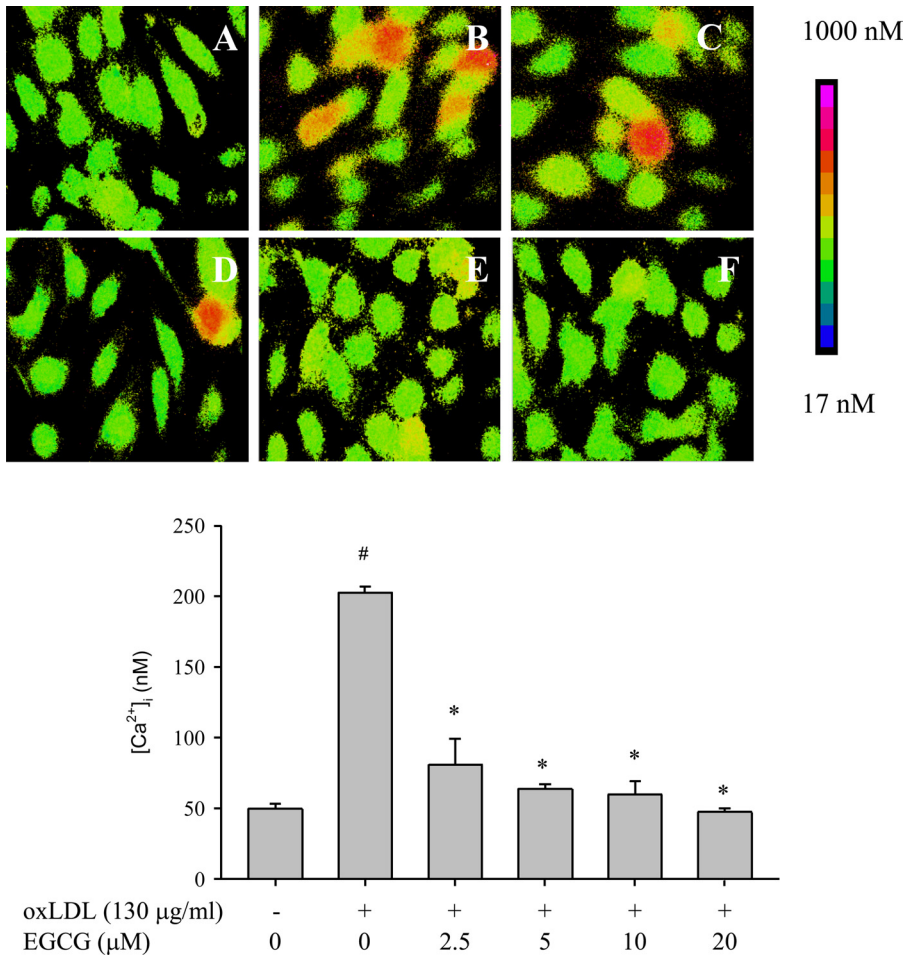

Fig. 7. Effect of EGCG on oxLDL-induced rise in cytoplasmic Ca^{2+} concentration ($[Ca^{2+}]_i$) in fura-2-loaded HUVECs. Images were processed as indicated in MATERIALS AND METHODS. Ca^{2+} changes are color coded (color bar) such that warm colors indicate high Ca^{2+} levels. *A*: no treatment. *B*: oxLDL treatment. *C*: oxLDL + 2.5 μM EGCG. *D*: oxLDL + 5 μM EGCG. *E*: oxLDL + 10 μM EGCG. *F*: oxLDL + 20 μM EGCG. Values are means ± SE of more than 250 individual cells from 3 separate experiments. #$P <$ 0.05 compared with untreated control HUVECs. *$P <$ 0.05 vs. oxLDL treatment.

ROS-sensitive signaling pathways (29). SOD protects against superoxide-mediated cytotoxicity by catalyzing O_2^- to form H_2O_2. However, H_2O_2 produced by dismutation of superoxide anion inactivates SOD-1. This process has been shown to play a key role in atherosclerosis (22). An increase in activity of SOD-1 prevents oxLDL-induced endothelial dysfunction (51). In support of findings from previous studies demonstrating that EGCG upregulates SOD-1 (28, 37), our data show that EGCG treatment significantly reduced the level of oxLDL-induced ROS generation (Fig. 2, *A* and *B*) and increased the level of SOD-1 expression (Fig. 2, *C* and *D*). We assume that EGCG protects against oxLDL-induced endothelial dysfunction by inhibiting LOX-1-mediated NADPH oxidase activation, thereby preserving H_2O_2-inactivated SOD-1. However, whether the effect of EGCG is solely due to its antioxidant activity has not been clearly elucidated. Our finding that the membrane translocation of $p47^{phox}$ and Rac-1 was reduced in cells pretreated with EGCG suggests that the effect of EGCG on NADPH oxidase is mediated by modulation of the assembly of $p47^{phox}$ and Rac-1 on the cell membrane (Fig. 3). The beneficial effect of EGCG might be due, at least in part, to suppression of the membrane assembly of the NADPH oxidase complex.

ROS can activate two signal transduction pathways involving either p38 MAPK or PI3K, both causing NF-κB activation and enabling nuclear translocation and subsequent regulation of proinflammatory molecules, including cytokines, chemokines, enzymes, and adhesion molecules (8). In the present study, ROS production in HUVECs occurred within 5 min (data not shown), and NF-κB was activated within 1 h of the addition of oxLDL. These data suggest that NF-κB activation follows the production of ROS in oxLDL-treated cells, which is consistent with the idea that ROS serves as a messenger of NF-κB activation. Therefore, one possible mechanism by which EGCG protects against oxLDL-induced endothelial dysfunction is blockade of the LOX-1-mediated signaling pathway, in which binding of oxLDL to LOX-1 activates the NADPH oxidase subunit p47 and Rac on the cell membrane, resulting in the quick increase of intracellular ROS and the subsequent activation of NF-κB via the p38 MAPK and PI3K pathways (Fig. 9).

In many vascular pathologies, a combination of altered rates of NO production along with an increased removal of NO leads to a reduction in the bioavailability of NO. The antithrombotic and antiatherosclerotic properties of NO are achieved by its ability to inhibit the expression of the cell surface adhesion molecules P-selectin, VCAM, and ICAM (25), prevent the expression of MCP-1 (58), and inhibit platelet adhesion under flow conditions (15). In normal physiology, superoxide is detoxified by the enzyme SOD, thereby preventing its interaction with NO. A recent study demonstrated that the PI3K/Akt pathway is an important upstream mediator of the NO/cGMP signals involved in the vasorelaxant action of EGCG in ophthalmic arteries (47). In the present study, we have demonstrated that EGCG ameliorated the oxLDL-diminished phos-

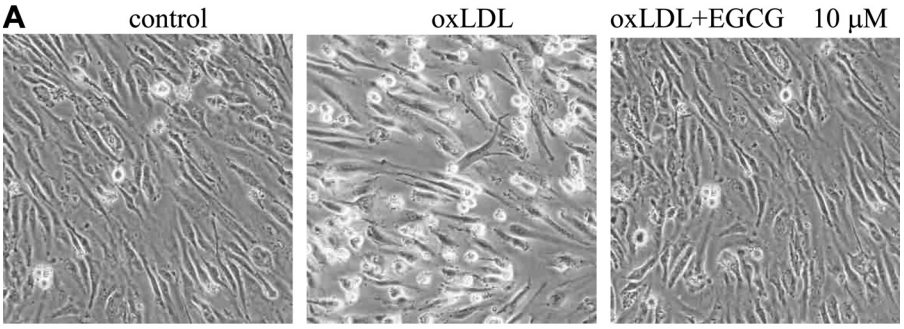

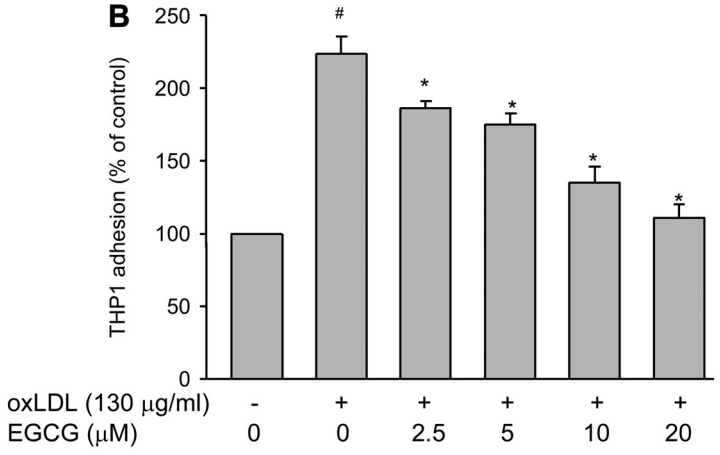

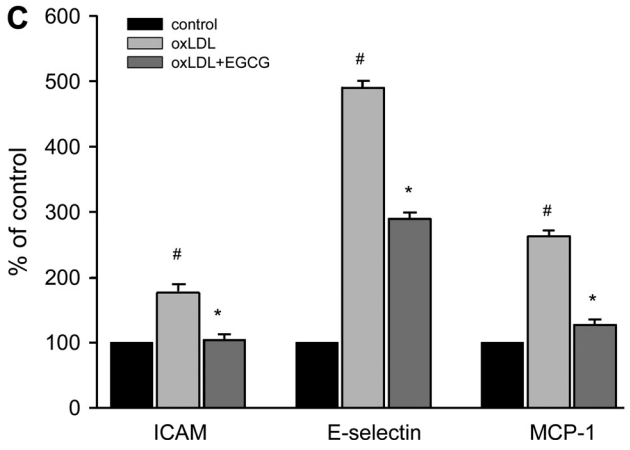

Fig. 8. Effects of EGCG on oxLDL-induced adhesion molecule expression and adhesiveness of THP-1 monocytic cells to HUVECs. Cells were incubated with the indicated concentrations of EGCG for 2 h and then incubated with oxLDL for an additional 24 h. *A* and *B*: dose-dependent effect of EGCG (2.5–20 μM) on oxLDL (130 μg/ml)-induced adhesiveness of THP-1 to HUVECs measured as described in MATERIALS AND METHODS. Values are means ± SE from 4 separate experiments. *$P < 0.05$ vs. oxLDL treatment. *C*: HUVECs were incubated with oxLDL (130 μg protein/ml) in the absence or presence of 20 μM EGCG (oxLDL+EGCG) for 24 h. The histogram of cell surface expression of ICAM-1, E-selectin, and monocyte chemoattractant protein-1 (MCP-1) was generated by flow cytometry. Values are means ± SE of 3 independent analyses. #$P < 0.05$ compared with untreated control HUVECs. *$P < 0.05$ vs. oxLDL treatment.

phorylation of Akt (Fig. 3, *A* and *C*) and increased the level of eNOS expression (Fig. 6), which contributed to the inhibition of oxLDL-induced adhesion of monocytes to HUVECs (Fig. 8, *A* and *B*). We further examined the inhibitory effects of EGCG on the oxLDL-induced surface expression of adhesion molecules in HUVECs. As expected, EGCG repressed the oxLDL-induced surface expression of these adhesion molecules (Fig. 8*C*). All of these findings strongly indicate that EGCG elicits antioxidative and anti-inflammatory effects. Our findings support those of previous reports demonstrating that the antioxidative effects of EGCG derive from its ability to inhibit ROS production via interaction with heme oxygenase-1 (55), thereby leading to the suppression of NADPH oxidase activation (42). With regard to the underlying mechanisms of anti-inflammation, EGCG inhibits angiotensin II-induced adhesion molecule expression (4) and acts as a potent inhibitor of NF-κB, a key transcription factor in the expression of inflammatory cytokines (41). In addition, recent studies have shown that EGCG improves endothelium-dependent vasodilation (23) and downregulates endothelial inflammatory parameters by modulating caveolae-regulated cell signaling (59). Together, these findings suggest that EGCG might play a role in the prevention of cardiovascular diseases.

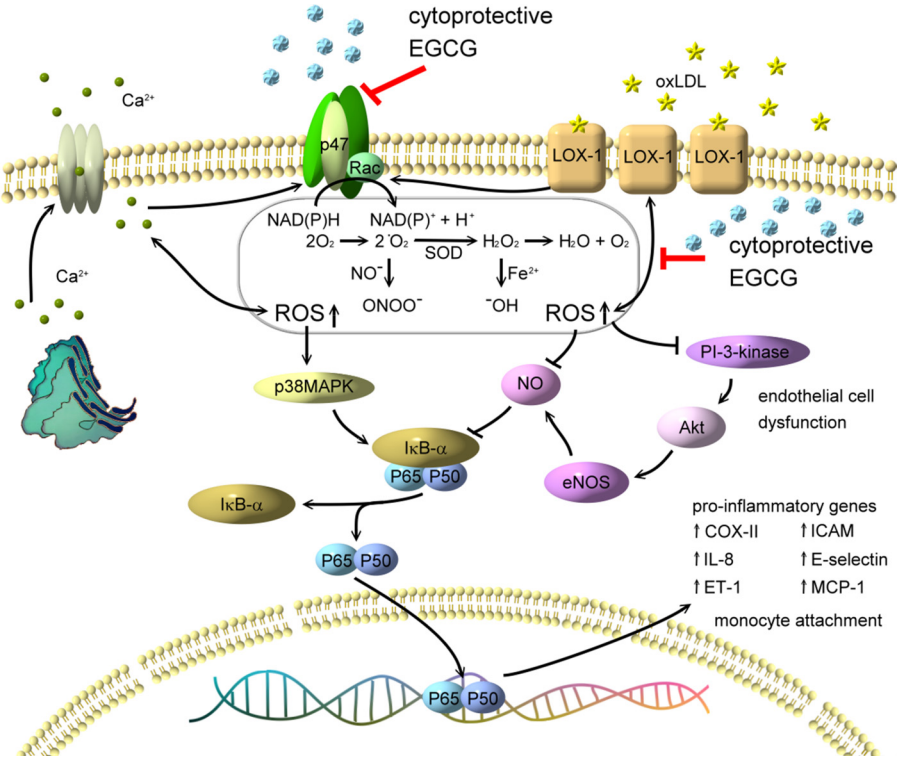

Fig. 9. Schematic diagram showing cytoprotective signaling of EGCG in oxLDL-induced endothelial dysfunction. As depicted, EGCG inhibits the LOX-1-mediated signaling cascades initiated by oxLDL-generated ROS. An arrowhead indicates activation or induction, and a vertical bar indicates inhibition or blockade.

Pathophysiological stimuli that induce endothelial activation via NADPH oxidase-mediated ROS-induced signal transduction and alteration of intracellular Ca^{2+} ion homeostasis are now considered to be major contributors to the pathogenesis of atherosclerotic coronary artery diseases (32). NADPH oxidase reportedly affects Ca^{2+} signaling in endothelial cells (21), and Ca^{2+} signaling regulates the membrane translocation and activation of Rac-1 and $p47^{phox}$ in response to certain agonists (45). Endothelial cells do not possess voltage-operated L-type Ca^{2+} channels. Matsui et al. (34) demonstrated that nifedipine, a Ca^{2+} channel blocker, decreased advanced glycation end product-induced MCP-1 overexpression by inhibiting ROS generation and subsequent NF-κB activation via suppression of NADPH oxidase. Our study found that ROS generation was the earliest signal and that it usually occurred within 5 min after the addition of oxLDL. Therefore, we assume that the antiatherogenic effects of EGCG are due to its ability to decrease the level of ROS generation, which aids in the maintenance of $[Ca^{2+}]_i$ in endothelial cells, thereby preventing the expression and adherence of monocytic THP-1 cells. In addition, oxLDL-induced increase in ROS preceded the increase in $[Ca^{2+}]_i$, suggesting that the increase in intracellular Ca^{2+} induced by oxidative stress may be a consequence of free radical action on Ca^{2+} ions stored in intracellular organelles.

OxLDL-induced O_2^- formation, which occurs largely through activation of NADPH oxidase but also through uncoupling of eNOS, xanthine oxidase, and peroxisomes and through direct O_2^- release, leads to endothelial dysfunction (17). In this regard, DPI has frequently been used to inhibit ROS production mediated by various flavoenzymes, including NADPH oxidase, quinone oxidoreductase, cytochrome *P*-450 reductase, and NOS (7, 13, 54). In the present study, we could not completely exclude the involvement of mitochondrial complex-1, which is also inhibited by DPI. On the other hand, our study showed that low-dose (5 μM) EGCG prevented the oxLDL-mediated assembly of NADPH oxidase, although the levels of LOX-1 expression and ROS generation remained high. Those findings indicate that low-dose EGCG might be sensitive enough to inhibit the membrane assembly of NADPH oxidase but not sensitive enough to inhibit the expression of other ROS-generating enzymes. We propose that partial activation of LOX-1 and the subsequent activation of a ROS-sensitive downstream pathway led to adhesion molecule expression and monocytic adherence.

The concentrations of EGCG (2.5–20 μM) used in our study are very similar to those used by researchers who reported that EGCG blocks LPS-induced inducible NOS expression (2.5–15 μM) (30), inhibits TNF-α-induced MCP-1 production (10–50 μM) (2), and inhibits oxLDL-induced endothelial apoptosis (25 μM) (10). In rats, the plasma concentration was reported to be as high as 12.3 μM at an oral dose of 500 mg/kg and 10.3 μM at an intravenous dose of 10 mg/kg (39). Metabolic studies in humans have shown that EGCG supplement is incorporated into plasma at a maximum concentration of 4,400 pmol/ml (40). Such concentrations would be enough to exert antioxidative activity in the bloodstream. Thus the concentrations of EGCG used in the present study are comparable to those achievable physiologically and to those used in animal studies.

In summary, EGCG prevents the oxLDL-induced LOX-1-mediated biological events that are closely linked to endothelial dysfunction. Because this is a purely in vitro work, further studies are required to confirm the extent to which EGCG inhibits oxLDL-mediated proatherogenic effects as well as the effectiveness of EGCG in vivo. Our findings add to the growing body of evidence for the beneficial effects of green tea consumption on improving cardiovascular health.

GRANTS

This study was supported by National Science Council Grants NSC 96-2320-B-235-001 and NSC 98-2320-B-039-020-MY3 and China Medical University Grant CMU98-N1-03, and Taiwan Department of Health Clinical Trial and Research Center of Excellence (DDHPP-TD-B-111-004) Taiwan, Republic of China.

DISCLOSURES

No conflicts of interest, financial or otherwise, are declared by the author(s).

REFERENCES

1. **Abo A, Pick E, Hall A, Totty N, Teahan CG, Segal AW.** Activation of the NADPH oxidase involves the small GTP-binding protein p21rac1. *Nature* 353: 668–670, 1991.
2. **Ahn HY, Xu Y, Davidge ST.** Epigallocatechin-3-*O*-gallate inhibits TNFα-induced monocyte chemotactic protein-1 production from vascular endothelial cells. *Life Sci* 82: 964–968, 2008.
3. **Bradford MM.** A rapid and sensitive method for the quantitation of microgram quantities of protein utilizing the principle of protein-dye binding. *Anal Biochem* 72: 248–254, 1976.
4. **Chae YJ, Kim CH, Ha TS, Hescheler J, Ahn HY, Sachinidis A.** Epigallocatechin-3-*O*-gallate inhibits the angiotensin II-induced adhesion molecule expression in human umbilical vein endothelial cell via inhibition of MAPK pathways. *Cell Physiol Biochem* 20: 859–866, 2007.
5. **Chen D, Milacic V, Chen MS, Wan SB, Lam WH, Huo C, Landis-Piwowar KR, Cui QC, Wali A, Chan TH, Dou QP.** Tea polyphenols, their biological effects and potential molecular targets. *Histol Histopathol* 23: 487–496, 2008.
6. **Chen J, Mehta JL, Haider N, Zhang X, Narula J, Li D.** Role of caspases in ox-LDL-induced apoptotic cascade in human coronary artery endothelial cells. *Circ Res* 94: 370–376, 2004.
7. **Chen L, Yu LJ, Waxman DJ.** Potentiation of cytochrome P450/cyclophosphamide-based cancer gene therapy by coexpression of the P450 reductase gene. *Cancer Res* 57: 4830–4837, 1997.
8. **Chen XP, Xun KL, Wu Q, Zhang TT, Shi JS, Du GH.** Oxidized low density lipoprotein receptor-1 mediates oxidized low density lipoprotein-induced apoptosis in human umbilical vein endothelial cells: role of reactive oxygen species. *Vascul Pharmacol* 47: 1–9, 2007.
9. **Chen XP, Zhang TT, Du GH.** Lectin-like oxidized low-density lipoprotein receptor-1, a new promising target for the therapy of atherosclerosis? *Cardiovasc Drug Rev* 25: 146–161, 2007.
10. **Choi JS, Choi YJ, Shin SY, Li J, Kang SW, Bae JY, Kim DS, Ji GE, Kang JS, Kang YH.** Dietary flavonoids differentially reduce oxidized LDL-induced apoptosis in human endothelial cells: role of MAPK- and JAK/STAT-signaling. *J Nutr* 138: 983–990, 2008.
11. **Cominacini L, Pasini AF, Garbin U, Davoli A, Tosetti ML, Campagnola M, Rigoni A, Pastorino AM, Lo Cascio V, Sawamura T.** Oxidized low density lipoprotein (ox-LDL) binding to ox-LDL receptor-1 in endothelial cells induces the activation of NF-κB through an increased production of intracellular reactive oxygen species. *J Biol Chem* 275: 12633–12638, 2000.
12. **Cominacini L, Rigoni A, Pasini AF, Garbin U, Davoli A, Campagnola M, Pastorino AM, Lo Cascio V, Sawamura T.** The binding of oxidized low density lipoprotein (ox-LDL) to ox-LDL receptor-1 reduces the intracellular concentration of nitric oxide in endothelial cells through an increased production of superoxide. *J Biol Chem* 276: 13750–13755, 2001.
13. **Cross AR, Jones OT.** The effect of the inhibitor diphenylene iodonium on the superoxide-generating system of neutrophils. Specific labelling of a component polypeptide of the oxidase. *Biochem J* 237: 111–116, 1986.
14. **Dandapat A, Hu C, Sun L, Mehta JL.** Small concentrations of oxLDL induce capillary tube formation from endothelial cells via LOX-1 dependent redox-sensitive pathway. *Arterioscler Thromb Vasc Biol* 27: 2435–2442, 2007.
15. **de Graaf JC, Banga JD, Moncada S, Palmer RM, de Groot PG, Sixma JJ.** Nitric oxide functions as an inhibitor of platelet adhesion under flow conditions. *Circulation* 85: 2284–2290, 1992.
16. **Tedeschi E, Suzuki H, Menegazz M.** Antiinflammatory action of EGCG, the main component of green tea, through STAT-1 Inhibition. *Ann NY Acad Sci* 973: 435–437, 2002.
17. **Galle J, Hansen-Hagge T, Wanner C, Seibold S.** Impact of oxidized low density lipoprotein on vascular cells. *Atherosclerosis* 185: 219–226, 2006.
18. **Grynkiewicz G, Poenie M, Tsien RY.** A new generation of Ca^{2+} indicators with greatly improved fluorescence properties. *J Biol Chem* 260: 3440–3450, 1985.
19. **Guo Q, Zhao B, Li M, Shen S, Xin W.** Studies on protective mechanisms of four components of green tea polyphenols against lipid peroxidation in synaptosomes. *Biochim Biophys Acta* 1304: 210–222, 1996.
20. **Havel RJ, Eder HA, Bragdon JH.** The distribution and chemical composition of ultracentrifugally separated lipoproteins in human serum. *J Clin Invest* 34: 1345–1353, 1955.
21. **Hu Q, Yu ZX, Ferrans VJ, Takeda K, Irani K, Ziegelstein RC.** Critical role of NADPH oxidase-derived reactive oxygen species in generating Ca^{2+} oscillations in human aortic endothelial cells stimulated by histamine. *J Biol Chem* 277: 32546–32551, 2002.
22. **Jewett SL, Rocklin AM, Ghanevati M, Abel JM, Marach JA.** A new look at a time-worn system: oxidation of CuZn-SOD by H_2O_2. *Free Radic Biol Med* 26: 905–918, 1999.
23. **Kim JA, Formoso G, Li Y, Potenza MA, Marasciulo FL, Montagnani M, Quon MJ.** Epigallocatechin gallate, a green tea polyphenol, mediates NO-dependent vasodilation using signaling pathways in vascular endothelium requiring reactive oxygen species and Fyn. *J Biol Chem* 282: 13736–13745, 2007.
24. **Kim JA, Territo MC, Wayner E, Carlos TM, Parhami F, Smith CW, Haberland ME, Fogelman AM, Berliner JA.** Partial characterization of leukocyte binding molecules on endothelial cells induced by minimally oxidized LDL. *Arterioscler Thromb* 14: 427–433, 1994.
25. **Kubes P, Suzuki M, Granger DN.** Nitric oxide: an endogenous modulator of leukocyte adhesion. *Proc Natl Acad Sci USA* 88: 4651–4655, 1991.
26. **Li D, Mehta JL.** Upregulation of endothelial receptor for oxidized LDL (LOX-1) by oxidized LDL and implications in apoptosis of human coronary artery endothelial cells: evidence from use of antisense LOX-1 mRNA and chemical inhibitors. *Arterioscler Thromb Vasc Biol* 20: 1116–1122, 2000.
27. **Li DY, Chen HJ, Mehta JL.** Statins inhibit oxidized-LDL-mediated LOX-1 expression, uptake of oxidized-LDL and reduction in PKB phosphorylation. *Cardiovasc Res* 52: 130–135, 2001.
28. **Li YM, Chen HY, Huang Y, Chen ZY.** Green tea catechins upregulate superoxide dismutase and catalase in fruit flies. *Mol Nutr Food Res* 51: 546–554, 2007.
29. **Lin SJ, Shyue SK, Liu PL, Chen YH, Ku HH, Chen JW, Tam KB, Chen YL.** Adenovirus-mediated overexpression of catalase attenuates oxLDL-induced apoptosis in human aortic endothelial cells via AP-1 and C-Jun N-terminal kinase/extracellular signal-regulated kinase mitogen-activated protein kinase pathways. *J Mol Cell Cardiol* 36: 129–139, 2004.
30. **Lin YL, Lin JK.** (−)-Epigallocatechin-3-gallate blocks the induction of nitric oxide synthase by down-regulating lipopolysaccharide-induced activity of transcription factor nuclear factor-kappa B. *Mol Pharmacol* 52: 465–472, 1997.
31. **Ludwig A, Lorenz M, Grimbo N, Steinle F, Meiners S, Bartsch C, Stangl K, Baumann G, Stangl V.** The tea flavonoid epigallocatechin-3-gallate reduces cytokine-induced VCAM-1 expression and monocyte adhesion to endothelial cells. *Biochem Biophys Res Commun* 316: 659–665, 2004.
32. **Madamanchi NR, Vendrov A, Runge MS.** Oxidative stress and vascular disease. *Arterioscler Thromb Vasc Biol* 25: 29–38, 2005.
33. **Marui N, Offermann MK, Swerlick R, Kunsch C, Rosen CA, Ahmad M, Alexander RW, Medford RM.** Vascular cell adhesion molecule-1 (VCAM-1) gene transcription and expression are regulated through an antioxidant-sensitive mechanism in human vascular endothelial cells. *J Clin Invest* 92: 1866–1874, 1993.
34. **Matsui T, Yamagishi S, Nakamura K, Inoue H, Takeuchi M.** Nifedipine, a calcium-channel blocker, inhibits advanced glycation end-product-induced expression of monocyte chemoattractant protein-1 in human cultured mesangial cells. *J Int Med Res* 35: 107–112, 2007.
35. **Mehta JL, Chen J, Yu F, Li DY.** Aspirin inhibits ox-LDL-mediated LOX-1 expression and metalloproteinase-1 in human coronary endothelial cells. *Cardiovasc Res* 64: 243–249, 2004.
36. **Mehta JL, Li D.** Identification, regulation and function of a novel lectin-like oxidized low-density lipoprotein receptor. *J Am Coll Cardiol* 39: 1429–1435, 2002.
37. **Meng Q, Velalar CN, Ruan R.** Effects of epigallocatechin-3-gallate on mitochondrial integrity and antioxidative enzyme activity in the aging process of human fibroblast. *Free Radic Biol Med* 44: 1032–1041, 2008.

38. **Nagase M, Ando K, Nagase T, Kaname S, Sawamura T, Fujita T.** Redox-sensitive regulation of LOX-1 gene expression in vascular endothelium. *Biochem Biophys Res Commun* 281: 720–725, 2001.
39. **Nakagawa K, Miyazawa T.** Absorption and distribution of tea catechin, (−)-epigallocatechin-3-gallate, in the rat. *J Nutr Sci Vitaminol (Tokyo)* 43: 679–684, 1997.
40. **Nakagawa K, Okuda S, Miyazawa T.** Dose-dependent incorporation of tea catechins, (−)-epigallocatechin-3-gallate and (−)-epigallocatechin, into human plasma. *Biosci Biotechnol Biochem* 61: 1981–1985, 1997.
41. **Navarro-Peran E, Cabezas-Herrera J, Sanchez-Del-Campo L, Garcia-Canovas F, Rodriguez-Lopez JN.** The anti-inflammatory and anticancer properties of epigallocatechin-3-gallate are mediated by folate cycle disruption, adenosine release and NF-kappaB suppression. *Inflamm Res* 57: 472–478, 2008.
42. **Nishikawa H, Wakano K, Kitani S.** Inhibition of NADPH oxidase subunits translocation by tea catechin EGCG in mast cell. *Biochem Biophys Res Commun* 362: 504–509, 2007.
43. **Nobuo S, Toshiyuki I, Koichi S, Tatsuya S, Takayuki S, Nobutaka I, Shu-ichi S, Masashi K, Hironori U, Hiroshi O, Koji S, Tamio T, Yukio M, Yasuchika T.** Role of LOX-1 in monocyte adhesion-triggered redox, Akt/eNOS and Ca^{2+} signaling pathways in endothelial cells. *J Cell Physiol* 220: 706–715, 2009.
44. **Ou HC, Chou FP, Sheu WH, Hsu SL, Lee WJ.** Protective effects of magnolol against oxidized LDL-induced apoptosis in endothelial cells. *Arch Toxicol* 81: 421–432, 2007.
45. **Price LS, Langeslag M, Klooster JP, Hedrick PL, Jilin K, Collard JG.** Calcium signaling regulates translocation and activation of Rac. *J Biol Chem* 278: 39413–39421, 2003.
46. **Reamers RA, Rice-Evans CA, Tyrrell RM, Clifford MN, Lean MEJ.** Tea flavonoids and cardiovascular health. *QJM* 94: 277–282, 2001.
47. **Romano MR, Logrono MD.** Epigallocatechin-3-gallate relaxes the isolated bovine ophthalmic artery: involvement of phosphoinositide 3-kinase-Akt-nitric oxide/cGMP signalling pathway. *Eur J Pharmacol* 608: 48–53, 2009.
48. **Rueckschloss U, Duerrschmidt N, Morawietz H.** NADPH oxidase in endothelial cells: impact on atherosclerosis. *Antioxid Redox Signal* 5: 171–180, 2003.
49. **Rueckschloss U, Galle J, Holtz J, Zerkowski HR, Morawietz H.** Induction of NAD(P)H oxidase by oxidized low-density lipoprotein in human endothelial cells: antioxidative potential of hydroxymethylglutaryl coenzyme A reductase inhibitor therapy. *Circulation* 104: 1767–1772, 2001.
50. **Sawamura T, Kume N, Aoyama T, Moriwaki H, Hoshikawa H, Aiba Y, Tanaka T, Miwa S, Katsura Y, Kita T, Masaki T.** An endothelial receptor for oxidized low-density lipoprotein. *Nature* 386: 73–77, 1997.
51. **Tang F, Wu X, Wang T, Wang P, Li R, Zhang H, Gao J, Chen S, Bao L, Huang H, Liu P.** Tanshinone II A attenuates atherosclerotic calcification in rat model by inhibition of oxidative stress. *Vascul Pharmacol* 46: 427–438, 2007.
52. **Tang WJ, Hu CP, Chen MF, Deng PY, Li YJ.** Epigallocatechin gallate preserves endothelial function by reducing the endogenous nitric oxide synthase inhibitor level. *Can J Physiol Pharmacol* 84: 163–171, 2006.
53. **Tipoe GL, Leung TM, Hung MW, Fung ML.** Green tea polyphenols as an anti-oxidant and anti-inflammatory agent for cardiovascular protection. *Cardiovasc Hematol Disord Drug Targets* 7: 135–144, 2007.
54. **Wever RMF, van Dam T, van Rijn HJM, de Groot F, Rabelink TJ.** Tetrahydrobiopterin regulates superoxide and nitric oxide generation by recombinant endothelial nitric oxide synthase. *Biochem Biophys Res Commun* 237: 340–344, 1997.
55. **Wu CC, Hsu MC, Hsieh CW, Lin JB, Lai PH, Wung BS.** Upregulation of heme oxygenase-1 by epigallocatechin-3-gallate via the phosphatidylinositol 3-kinase/Akt and ERK pathways. *Life Sci* 78: 2889–2897, 2006.
56. **Xu H, Duan J, Wang W, Dai S, Wu Y, Sun R, Ren J.** Reactive oxygen species mediate oxidized low-density lipoprotein-induced endothelin-1 gene expression via extracellular signal-regulated kinase in vascular endothelial cells. *J Hypertens* 26: 956–963, 2008.
57. **Xu H, Lui WT, Chu CY, Ng PS, Wang CC, Rogers MS.** Anti-angiogenic effects of green tea catechin on an experimental endometriosis mouse model. *Hum Reprod* 24: 608–618, 2009.
58. **Zeiher AM, Fisslthaler B, Schray-Utz B, Busse R.** Nitric oxide modulates the expression of monocyte chemoattractant protein 1 in cultured human endothelial cells. *Circ Res* 76: 980–986, 1995.
59. **Zheng Y, Lim EJ, Wang L, Smart EJ, Toborek M, Hennig B.** Role of caveolin-1 in EGCG-mediated protection against linoleic-acid-induced endothelial cell activation. *J Nutr Biochem* 20: 202–209, 2009.